Puncture Deformation and Fracture Mechanism of Oriented Polymers

Y. Yang,[1] M. Ponting,[1] G. Thompson,[2] A. Hiltner,[1] E. Baer[1]

[1]*Center for Applied Polymer Research, Macromolecular Science and Engineering Department, Case Western Reserve University, Cleveland, Ohio 44106-7202*
[2]*U.S. Army Dental and Trauma Research Detachment, 310B B Street, Building 1H, Great Lakes, Illinois 60088-5259*

Received 6 November 2010; accepted 1 January 2011
DOI 10.1002/app.34109
Published online 2 November 2011 in Wiley Online Library (wileyonlinelibrary.com).

ABSTRACT: In this study, we investigated the effect of orientation by solid-state cross-rolling on the morphology, puncture deformation, and fracture mechanism of an amorphous TROGAMID material and three semicrystalline polymers: high-density polyethylene (HDPE), polypropylene (PP), and nylon 6/6. In amorphous TROGAMID, it was found that orientation preferentially aligned polymer chains along the rolling deformation direction and reduced the plastic deformation of TROGAMID in a low-temperature puncture test. The decrease of ductility with orientation changed the fracture mechanism of TROGAMID from ductile hole enlargement failure in the unoriented control to a more brittle delamination failure in TROGAMID cross-rolled to a 75% thickness reduction. For semicrystalline polymers HDPE, PP, and nylon 6/6, the randomly oriented crystalline lamellae in the controls were first oriented into an oblique angle to the rolling direction (RD) before the lamellae became fragmented and preferentially oriented with the chain axis parallel to the RD. The morphological change resulted in the decrease of ductility in HDPE in the low-temperature puncture test. In PP and nylon 6/6, the brittle fracture of unoriented controls was changed into ductile failure when they were cross-rolled to a 50% thickness reduction. This was attributed to the tilted crystal lamellae morphology, which permitted chain slip deformation of crystals with the chain axis parallel to the maximum shear stress direction. With further orientation of PP and nylon 6/6 to a 75% thickness reduction, the failure mechanism changed back to brittle fracture as the morphology transformed into a layered discoid structure with the chain axis of the fragmented crystal blocks parallel to the RD; this prevented chain slip deformation of the crystals. J Appl Polym Sci 124: 2524–2536, 2012

Key words: brittle; ductile; fracture; morphology; orientation

INTRODUCTION

Orientation has been widely used to improve the strength and toughness of polymers.[1] With preferential alignment of the polymer chains, segments of the polymer chains, or the crystalline regions in the polymers, the stiffness and strength of polymers can be greatly improved in the orientation direction.[2–5] The orientation of polymers can be conducted either from the molten or dissolved state or from the solid state by rolling, compression, or drawing deformation. Because of their remarkable drawability, semicrystalline polymers have attracted great interest, as they can be highly oriented in the solid state to generate highly anisotropic properties. Semicrystalline polymers often form a spherulitic structure with crystal lamellae randomly distributed in the spherulites and connecting amorphous phase in between the crystal lamellae. In the orientation of semicrystalline polymers by solid-state deformation, the spherulitic structure will be gradually changed into a microfibrillar structure through structural changes in various levels, including deformation of spherulites, rotation of lamellae, deformation of the crystal lattice, unfolding of chains in the crystals, and straightening of the random-chain configuration in the amorphous phase. Compared to semicrystalline polymers, amorphous polymers do not possess a structure of long-range three-dimensional order, although some degree of short-range order in the form of coil or bundle structures does exist.[6,7] In order to manipulate the final properties of oriented polymers by controlling the orientation state of the crystal lamellae and amorphous phase.[8] To control the orientation state of the crystal lamellae and amorphous phase to manipulate the final properties of oriented polymers, it is important to understand the microstructure or morphological change during the orientation process. On the other hand, the complex problem of structural change in different dimensional levels during the plastic deformation process of polymers has also been of intense interest

Correspondence to: Y. Yang (yxy60@case.edu).

for academic research. Thus, it is not surprising that a large amount of research has been conducted in this area.[9–12]

The toughness of polymers is closely related to their ability to undergo plastic deformation without failure. Depending on whether the polymer fails with or without plastic deformation, two principal modes of polymer behavior can be categorized: brittle, characterized by a short, nearly linear relationship between load and displacement, and ductile, characterized by yielding and plastic flow. In crystalline polymers, the structure consists of chain-folded crystalline lamellae and an interlamellar amorphous phase. The crystalline structure has a three-dimensional order, which severely constrains the motion of polymer chains in crystals. Because the yielding of crystalline polymers is primarily of a crystal plasticity nature involving chain sliding on one or more crystallographic planes,[13,14] the toughness of crystalline polymers will be greatly affected by the orientation of the crystalline phase, as the chain sliding motion is more feasible in the chain-axis direction than the other directions. On the other hand, amorphous polymers do not possess a three-dimensional order crystalline structure, and the yielding of amorphous polymers is attributed to the localized shear deformation of chain clusters.[13,15] Orientation of amorphous polymers will cause the coiled chain segments to become straightened and, thereby, affect their ability to undergo plastic deformation; this will affect the toughness of amorphous polymers. Therefore, it is also important to understand the relationship between the microstructural change and the macromechanical behavior to improve the toughness of oriented polymers.

The microstructural change with orientation can also affect the fracture mechanisms of polymers. For example, Sova et al.[16] found that the orientation of polypropylene (PP) composite materials improved the resistance to crack propagation because of the crack blunting effect, which greatly increased the impact energy absorption. Snyder et al.[17] showed that in a low-temperature tensile test, the failure mechanism of biaxially oriented PP changed from a brittle craze fracture into a ductile delamination failure with orientation changing the spherulitic structure into a layered discoid structure. So by studying the fracture damage zones and the failure mechanism, one can also elucidate information on the morphological change in the orientation process.

In a previous publication,[18] we discussed the effect of orientation on the microstructure of several semicrystalline polymers and its relationship to the macromechanical properties, including the modulus, yield stress, and strain-hardening exponent in uniaxial tensile tests. In this study, we investigated the effect of orientation on the puncture deformation and fracture mechanisms of an amorphous TROGAMID material and three semicrystalline polymers, high-density polyethylene (HDPE), PP, and nylon 6/6, at a low temperature of −40°C. The puncture performance and fracture mechanisms of the oriented polymers were then examined with the microstructure and morphology at different orientation states.

EXPERIMENTAL

Materials

One amorphous TROGAMID material and three semicrystalline polymers, HDPE, PP, and nylon 6/6, were used in this study. Table I lists some properties for the materials used in this study. The TROGAMID sheets were obtained from injection-molded sheets of an aliphatic polyamide, TROGAMID CX7323, supplied by Evonik Industries AG (Essen, Germany). Biaxial orientation of TROGAMID sheets were conducted by solid-state cross-rolling. Samples were first heated to 100°C in an oven before being cross-rolled. The sample was then pushed through the gap of two rotating rolls. As the sample thickness was larger than the gap of these two rolls, the sample was compressively sheared. Then, the gap was decreased by 0.127 mm (5 mil) and the sample was rotated 90° for the next rolling pass to achieve biaxial orientation. The process was repeated many times until the desired thickness was reached. The detailed cross-rolling process was described in a previous publication.[19] Two cross-rolling thickness reductions were used in this study, 50 and 75%, which corresponded to draw ratios of 1.4 × 1.4 and 2 × 2.

The three semicrystalline polymers, HDPE, PP, and nylon 6/6, used in this study were described in a previous publication.[18] All polymer sheets were biaxially oriented with a solid-state cross-rolling technique. Two oriented samples were prepared in this study; one had a 50% cross-rolling thickness reduction, and the other had a 75% cross-rolling

TABLE I
List of Some Properties for the Materials Used in this Study

Material	T_g (°C)	β relaxation (°C)	Melting temperature (°C)	X_c (%)
TROGAMID	150	−55	245	~ 5[a]
HDPE	−77[b]	–	132	~ 75
PP	0	–	160	~ 45
Nylon 6/6	50	–	256	~ 30

[a] Crystallinity (X_c) of TROGAMID was estimated from the differential scanning calorimetry thermogram as heat of fusion (ΔH) ≈ 10 J/g.
[b] Listed as the brittle temperature by the manufacturer.

thickness reduction. An unoriented sample with the same thickness was used as the control for this investigation.

Wide-angle X-ray scattering (WAXS) and small-angle X-ray scattering (SAXS)

The structure and global orientation of the cross-rolled polymer sheets were examined by two-dimensional (2D) WAXS and SAXS measurements with a rotating anode X-ray generator (Rigaku RU 300, 12kW) (Tokyo, Japan). To collect 2D WAXS images, a collimated X-ray beam with a 1-mm diameter was irradiated in the direction parallel to the rolling direction (RD) or the ND of the polymer sheets, and the scattered beam was recorded with a Bruker Hi-Star detector (Billerica, MA). 2D SAXS was done with a Rigaku S-Max3000 pinhole camera, which gave a highly focused parallel beam of monochromatic Cu Kα radiation ($\lambda = 0.154$ nm) and was equipped with a 2D gas-filled multiwire detector. The X-ray exposure time was 20 min for WAXS and 30 min for SAXS. Because the samples were equally oriented in two cross-rolling directions and the WAXS and SAXS images measured along the two RDs were identical to each other without discernable differences, only one of the two RD X-ray patterns is shown.

Dynamic mechanical thermal analysis (DMTA)

The effect of orientation on the dynamic mechanical properties was measured with a Q800 dynamic mechanical analyzer from TA Instruments (New Castle, DE). Specimens were tested in the dynamic tensile mode with a frequency of 1 Hz and a strain of 0.1%. The test temperature ranged from −100 to 200°C with a heating rate of 3°C/min for the amorphous TROGAMID.

Low-temperature puncture test

The effect of orientation on the puncture resistance of these four polymers was evaluated with a low-temperature puncture test. The tests were performed on a hydraulic Instron (Norwood, MA) model 8500 instrument with a 10-kN load cell. The specimens were cut into 63.5 ×63.5 mm^2 squares with an electric bandsaw. The specimens were then fixed by a metal clamp before being put into an environment chamber to be cooled to the set temperature of −40°C. After the set temperature was reached, an additional 15 min was allowed for the temperature to equilibrate. A North Atlantic Treaty Organization (NATO) standard 9-mm ball design puncture head was used, and the tests were conducted with a crosshead speed of 10 m/min. Figure 1 shows a schematic of the puncture test setup.

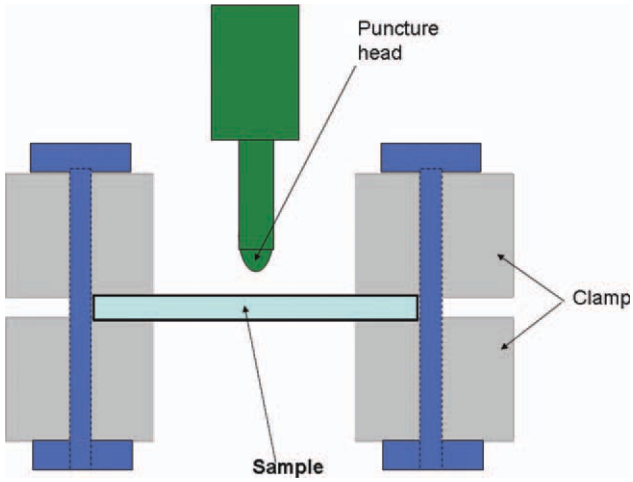

Figure 1 Schematic of the puncture test setup: the test specimen was fixed with a metal clamp and punctured at the center. The crosshead speed used for the test was 10 m/min. [Color figure can be viewed in the online issue, which is available at wileyonlinelibrary.com.]

Damage zone analysis

The puncture fracture damage zones were imaged and analyzed from both the top view and the side view with a digital camera, optical microscopy, and scanning electron microscopy (SEM). For the top-view analysis, an Olympus C-5050ZOOM digital camera (Center Valley, PA) was used. For the side-view analysis, the specimens were cut through the damage zone center and polished with 1200-grit sandpaper. The specimens were then analyzed with an Olympus BH-2 optical microscope (Center Valley, PA) in reflection mode. For SEM analysis, a JEOL JSM 840A scanning electron microscope (Tokyo, Japan) was used. Specimens were coated with 16 nm of gold before being observed with SEM. The SEM accelerator voltage was maintained at 25 kV, and the probe current was 6×10^{-11} A.

RESULTS AND DISCUSSION

Effect of orientation on the morphology of amorphous TROGAMID and the three semicrystalline polymers

The effect of orientation on the structure of amorphous TROGAMID was studied with 2D wide-angle X-ray diffraction and DMTA. Figure 2(a) compares the 2D WAXS patterns of TROGAMID rolled to different thickness reductions. The pattern of the unoriented CX7323 control exhibited a diffuse ring reflection from an amorphous halo. The isotropic ring pattern indicated that amorphous chains were randomly distributed without a preferred orientation in the unoriented control. The ring pattern was replaced by a broad two-arc reflection in the meridian region in the WAXS pattern of TROGAMID

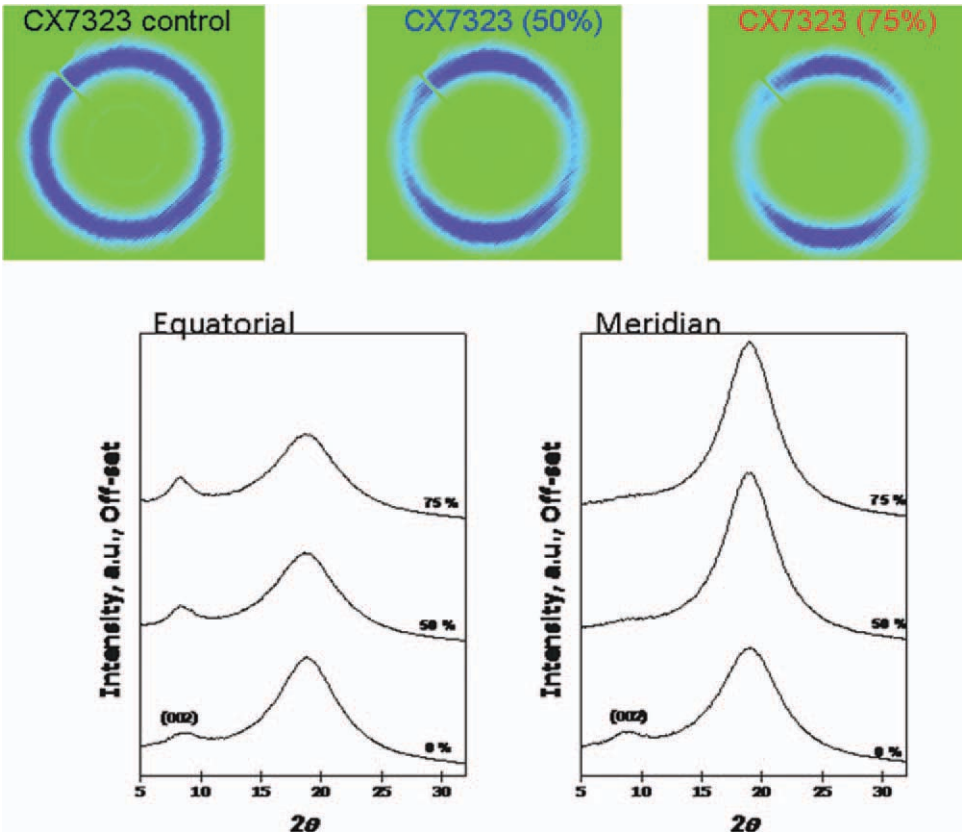

Figure 2 2D WAXS patterns (top) and azimuthal intensity scan (bottom) of the cross-rolled TROGAMID. The X-ray beam was aligned parallel to the plane of sheets, and the cross-rolling direction was horizontal in the X-ray images. The amount of thickness reduction is also indicated. [Color figure can be viewed in the online issue, which is available at wileyonlinelibrary.com.]

rolled to a 50% thickness reduction; this suggested that the molecular chains were preferentially oriented along the RD.[20,21] The two-arc pattern became sharper and shorter with TROGAMID rolled to a 75% thickness reduction; this indicated a higher degree of molecular chain orientation in the RD. Figure 2(b) shows the effect of orientation on the amorphous halo reflection intensity in the equatorial and meridian regions. The intensity in the equatorial region decreased with increasing orientation, whereas the intensity in the meridian region increased with increasing orientation; this indicated a higher degree of amorphous chain orientation in the RD with a larger rolling thickness reduction.

The orientation structure of amorphous TROGAMID was further studied with DMTA. Figure 3 shows a comparison of the DMTA tan δ curves of TROGAMID cross-rolled to different thickness reductions. The intensity of tan δ decreased with increasing orientation, whereas the tan δ peak shifted to a higher temperature from 136°C for the control to 144°C for TROGAMID CX7323 (75%). The decrease of the tan δ peak and shift to a higher temperature was attributed to the decrease in chain mobility with increasing orientation, as amorphous tie chains became more and more stretched with rolling orientation. Similar results were previously reported for the orientation of PP.[22,23] This further confirmed the orientation of amorphous chains in the RD.

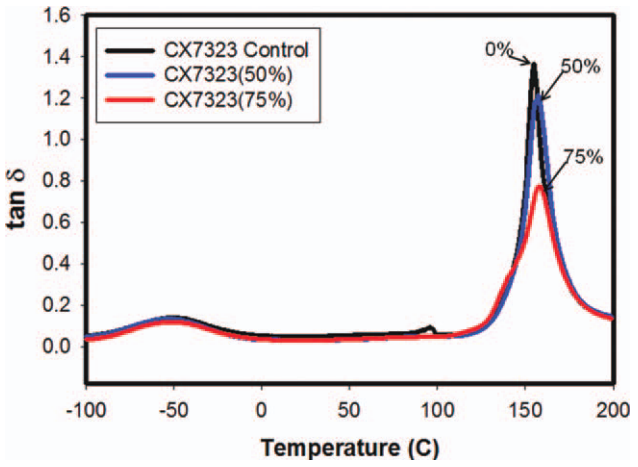

Figure 3 DMTA tan δ curve comparison of TROGAMID rolled to different thickness reductions. The test was conducted in the tensile mode with a frequency of 1 Hz and a heating rate of 3°C/min from −100 to 200°C. [Color figure can be viewed in the online issue, which is available at wileyonlinelibrary.com.]

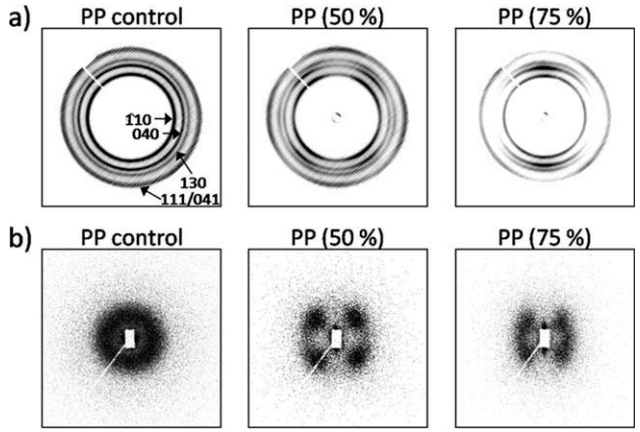

Figure 4 (a) 2D WAXS and (b) 2D SAXS patterns of the cross-rolling biaxially oriented PP sheets from the side view. The X-ray beam was aligned parallel to the plane of sheets, and the cross-rolling direction was horizontal in the X-ray images. The amount of thickness reduction and the Miller indices are indicated.

Compared with amorphous TROGAMID, the structural change of the crystalline polymers with orientation was more complicated, as it involved the deformation and orientation of both the crystalline and amorphous phases. Figure 4 shows the structural characterization with WAXS and SAXS of PP rolled to different thickness reductions. Both the WAXS and SAXS patterns of the unoriented PP control exhibited an isotropic ring reflection; this indicated that the crystal lamellae were randomly distributed. The WAXS pattern of PP rolled to a 50% thickness reduction showed a four-arc pattern at the off axis from the reflection of planes (110), (040), and (130) and a four-arc pattern at the equator and meridian from the reflection of plane (111/041), whereas the SAXS pattern exhibited a four-point reflection at the off axis. This indicated that the crystal lamellae were oriented at an oblique angle to the RD. With PP further oriented to a 75% thickness reduction, the WAXS pattern exhibited a two-arc pattern in the meridian from the reflection of planes (110), (040), and (130) and a four-arc off-axis reflection from plane (111/041), whereas the four-point reflection in the SAXS pattern became sharper. The WAXS and SAXS patterns implied that the crystal lamellae became fragmented into crystal blocks with the chain axis of crystal blocks being parallel to the RD. The orientation of crystalline lamellae was accompanied by the orientation of the amorphous phase. Figure 5 shows the comparison of a profile-fitted radial scan in the equatorial and meridian regions for PP rolled to different thickness reductions. In the equatorial region, the intensity of the amorphous halo decreased with increasing cross-rolling, whereas in the meridian region, the intensity of the amorphous halo increased with increasing cross-rolling. This indicated that the amorphous chains in the semicrystalline polymers were preferentially oriented in the RD along with the orientation of crystalline phase. Similar results were observed in the cross-rolling orientation of HDPE and nylon. Randomly distributed crystal lamellae in the unoriented control samples first became tilted to the RD with cross-rolling deformation before they became oriented with the chain axis parallel to the

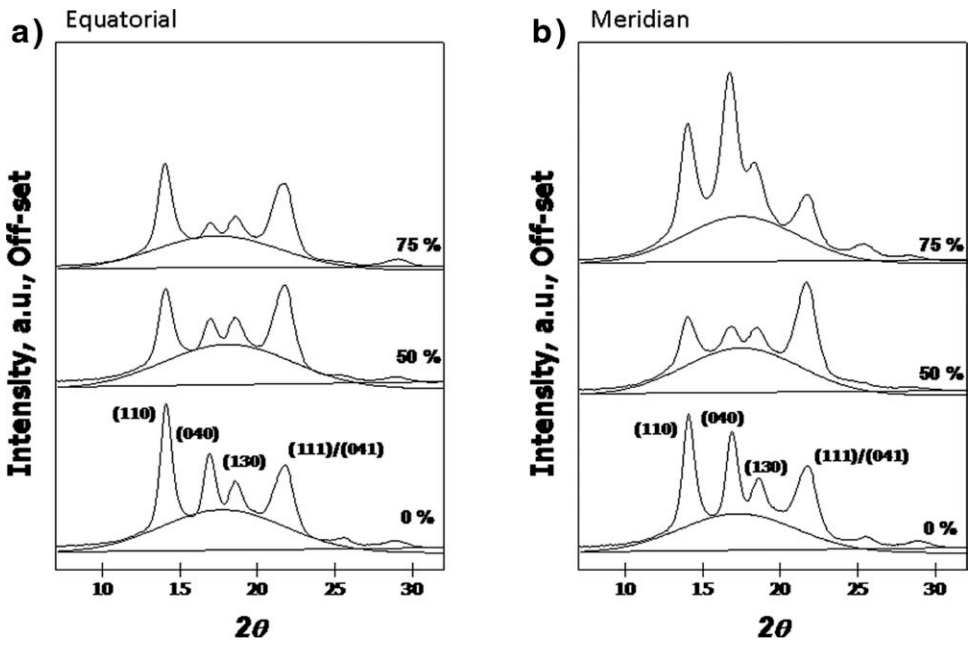

Figure 5 Effect of orientation on the profile-fitted amorphous intensity of PP in the (a) equatorial and (b) meridian regions.

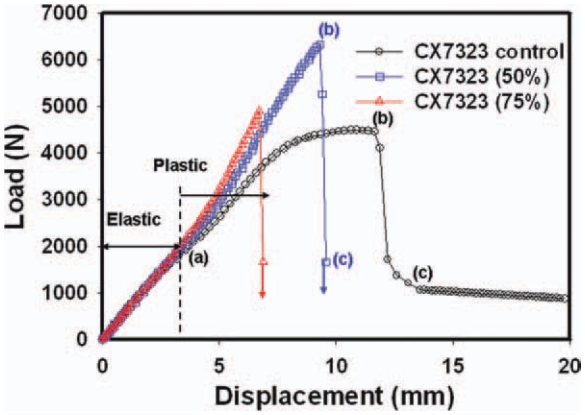

Figure 6 Effect of orientation on the puncture load–displacement curve of TROGAMID. The test was conducted at −40°C with a crosshead speed of 10 m/min: (a) elastic, (b) plastic, and (c) residual friction regions of the load–displacement curve. [Color figure can be viewed in the online issue, which is available at wileyonlinelibrary.com.]

RD when being further cross-rolled. A more thorough discussion about the structural change of crystalline polymers with orientation can be found in a previous publication.[18]

Effect of orientation on the puncture performance of amorphous and crystalline polymers

The effect of microstructural change on the macromechanical properties of the oriented polymers was studied with a low-temperature puncture test. Figure 6 shows the puncture load–displacement curves of TROGAMID rolled to different thickness reductions. All TROGAMID samples exhibited ductile failure with plastic deformation, regardless of the degree of orientation. Although the glass-transition temperature (T_g) of TROGAMID was around 150°C, it showed a low-temperature β transition at about −55°C, and its polymer chains still possessed some mobility at the test temperature of −40°C; this allowed the samples to have plastic deformation before the occurrence of fracture. Similar to the puncture of fiber-reinforced composites,[24,25] three regions could be identified on the load–displacement curves: the elastic region, the plastic region, and the fracture region. In the elastic region, where the deformation was elastic and could recover completely with the load removed, the slope of the load–displacement curve was about the same as the modulus did not significantly changed with orientation.[19] However, in the plastic region, where irreversible permanent deformation occurred, the slope of the load–displacement curve increased with increasing orientation. This was attributed to the increased strain-hardening exponent with oriented TROGAMID as the chain entanglement network became stretched by the rolling orientation. Further depression of the puncture tip into the specimen caused the distal surface to start cracking from tensile stress with fracture propagating through the whole sample thickness. This region was designated as the fracture propagation region. The fracture displacement of TROGAMID decreased with increasing orientation from 11.7 mm for the unoriented control to 6.7 mm for TROGAMID cross-rolled to a 75% thickness reduction. The decreased plasticity of TROGAMID with orientation was due to the fact that orientation straightened the polymer chains and preferentially aligned them to the RD. Because the plasticity of amorphous polymers originated from the relaxation of chain clusters in the range of 8–10 nm,[13] this led to the decreased ductility of amorphous TROGAMID with increasing degree of orientation.

The effect of orientation on the puncture load–displacement curves of crystalline HDPE is shown in Figure 7. Similar to amorphous TROGAMID, all HDPE samples exhibited plastic deformation, regardless of the degree of orientation, as the test temperature was still above the T_g of HDPE and the polymer chains were in a rubbery state. The slope of the load–displacement curves of HDPE in the elastic region also did not change with orientation as the elastic modulus remained unchanged. However, the slope of the load–displacement curve in the plastic region increased with increasing orientation because the stretched chain network led to an increased strain-hardening exponent. The increase of the strain-hardening exponent increased the peak load from 3830 N for the unoriented HDPE control to 5400 N for HDPE (75%; Table II). Unlike amorphous

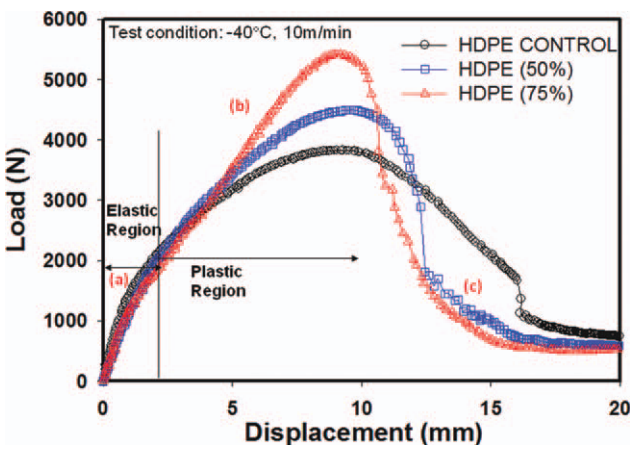

Figure 7 Effect of orientation on the puncture load–displacement curve of HDPE. The test was conducted at −40°C with a crosshead speed of 10 m/min: (a) elastic, (b) plastic, and (c) residual friction regions of the load–displacement curve. [Color figure can be viewed in the online issue, which is available at wileyonlinelibrary.com.]

TABLE II
Effect of the Orientation on the Puncture Performance of Various Polymers

Material		Peak load (N)	Fracture displacement (mm)	Energy absorption (J)
TROGAMID	Control	4480	11.7	33.7
	50%	6320	9.3	27.6
	75%	4900	6.7	14.6
HDPE	Control	3830	16.0	45.9
	50%	4500	12.3	40.3
	75%	5420	10.6	37.1
PP	Control	2610	1.3	2.0
	50%	5580	16.1	63.2
	75%	2190	1.1	1.2
Nylon 6/6	Control	1290	1.4	0.8
	50%	7210	11.9	50.8
	75%	960	1.1	0.5

TROGAMID, where the load exhibited a steep drop after the peak load, the load showed a more gradual decrease after the peak load. This gradual drop of load was attributed to the decrease of sample thickness from the plastic membrane stretching instead of the initiation of fracture. A sudden drop in the load was observed at higher displacement, which corresponded to the initiation of fracture in the specimen. As in the case of TROGAMID, the fracture displacement also decreased with increasing orientation for HDPE, changing from 16.0 mm for the unoriented control to 10.6 mm for HDPE (75%) because of previous stretching of the polymer chains from the rolling orientation.

Figure 8 shows the effect of orientation on the puncture load–displacement curves of PP. Compared with HDPE, PP had a higher T_g, at approximately

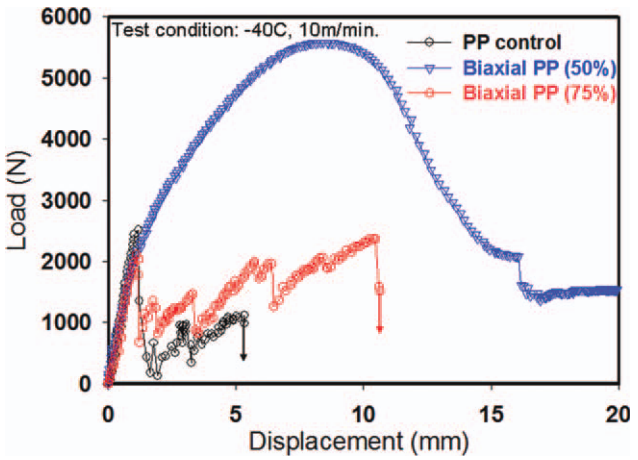

Figure 8 Effect of orientation on the puncture load–displacement curve of PP. The test was conducted at −40°C with a crosshead speed of 10 m/min. [Color figure can be viewed in the online issue, which is available at wileyonlinelibrary.com.]

0°C. At −40°C, the polymer chains were in glassy state; this led to the brittle fracture of the unoriented PP control without plastic deformation. Multiple peaks were observed in the load–displacement curve as the specimen shattered in a glasslike brittle fracture.[26] The brittle fracture was transitioned into a ductile failure with large plastic deformation, as PP was oriented to a 50% cross-rolling thickness reduction. The fracture displacement increased from 1.3 mm for the control to 16.1 mm for the 50% oriented PP, and the fracture energy increased by a factor of 30 from 2.0 to 63.2 J (Table II). For semicrystalline polymers, the plasticity is primarily due to the plastic deformation of crystals.[13,27] With PP rolled to a 50% thickness reduction, the randomly distributed

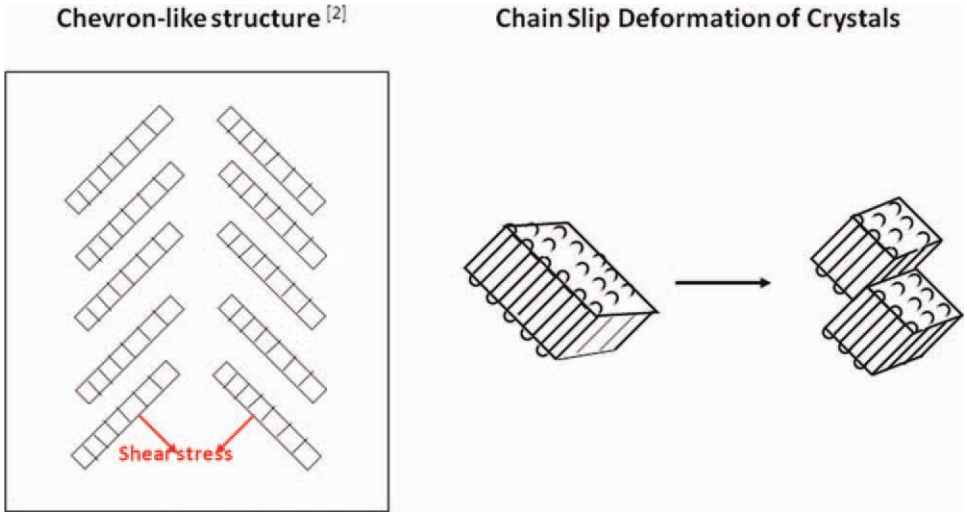

Figure 9 Schematic of the tilted lamellar structure in PP rolled to a 50% thickness reduction and chain slip deformation of the tilted crystal lamellae. [Color figure can be viewed in the online issue, which is available at wileyonlinelibrary.com.]

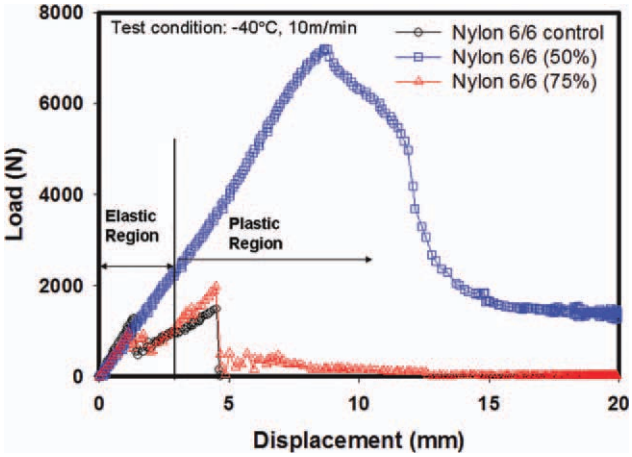

Figure 10 Effect of orientation on the puncture load–displacement curve of nylon 6/6. The test was conducted at −40°C with a crosshead speed of 10 m/min. [Color figure can be viewed in the online issue, which is available at wileyonlinelibrary.com.]

lamellae of the spherulitic structure were changed to a tilted lamellar structure with the chain axis of the crystals aligned about 45° to the RD. With the chain axis parallel to the puncture shear stress direction, the crystals could be plastically deformed by the chain slip deformation mechanism, even though the temperature was below the T_g of PP and the chain mobility was greatly reduced. Figure 9 shows a schematic of the tilted lamellar structure of PP rolled to a 50% thickness reduction and the chain slip deformation of tilted lamellae under puncture shear stress. When the orientation of PP was further increased to a 75% thickness reduction, the tilted lamellar structure was replaced by a microfibrillar structure with the chain axis of the crystals parallel to the RD. This prevented the chain slip deformation of crystals and resulted in the brittle failure of PP rolled to a 75% thickness reduction. Multiple peaks were also observed in the load–displacement curve of 75% oriented PP; this was a result of delamination from the layeredlike discoid structure similar to the puncture of layered laminates.[24]

The effect of orientation on the puncture behavior of nylon 6/6 (shown in Fig. 10) was similar to PP. The unoriented control of nylon 6/6 showed brittle fracture without plastic deformation as the test temperature was below the T_g of nylon 6/6, and the amorphous chains were in a glassy state. With a 50% thickness reduction, ductile failure with a large plastic deformation was observed. The fracture displacement was increased by a factor of 8, and the energy absorption was increased by a factor of 50 compared to the unoriented control (Table II); this was attributed to the tilted lamellar structure, which allowed chain slip deformation of the crystals. Further cross-rolling of nylon 6/6 to a 75% thickness reduction resulted in crystal block oriented with the chain axis parallel to the RD; this prohibited chain slip deformation of the crystals in

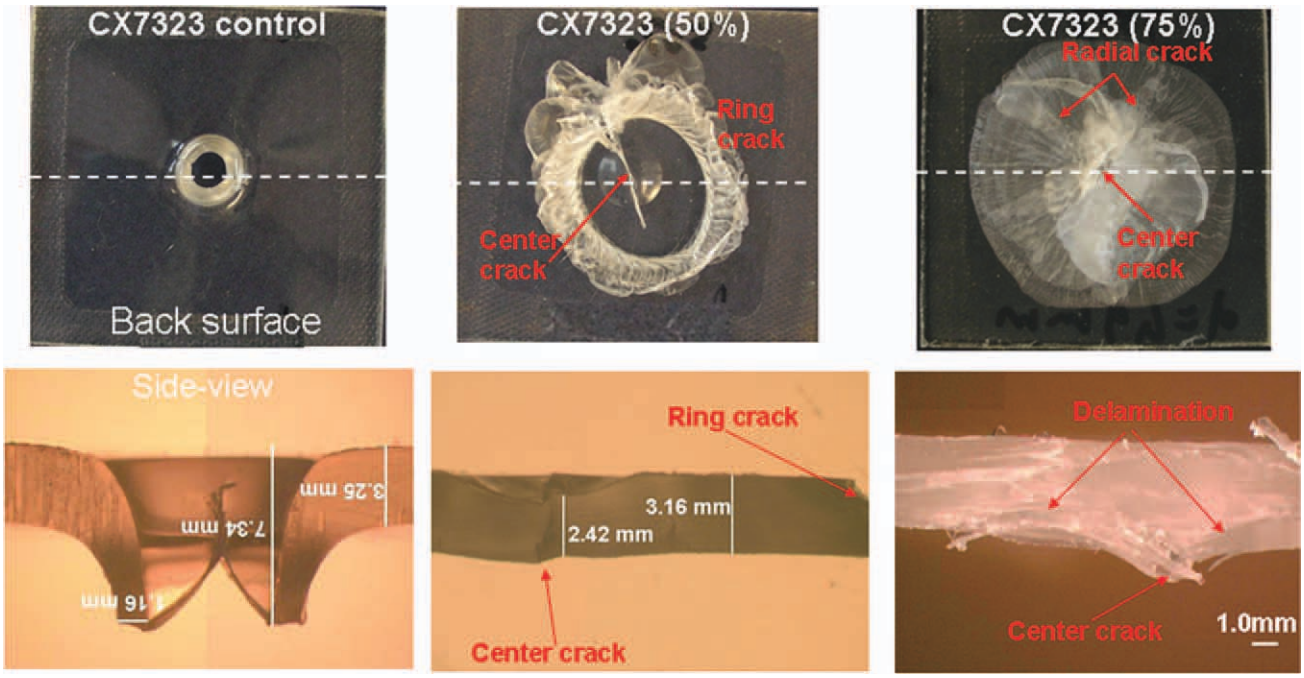

Figure 11 Effect of orientation on the puncture fracture damage zones of TROGAMID: (a) top view and (b) cross-sectional view of the damage zone. [Color figure can be viewed in the online issue, which is available at wileyonlinelibrary.com.]

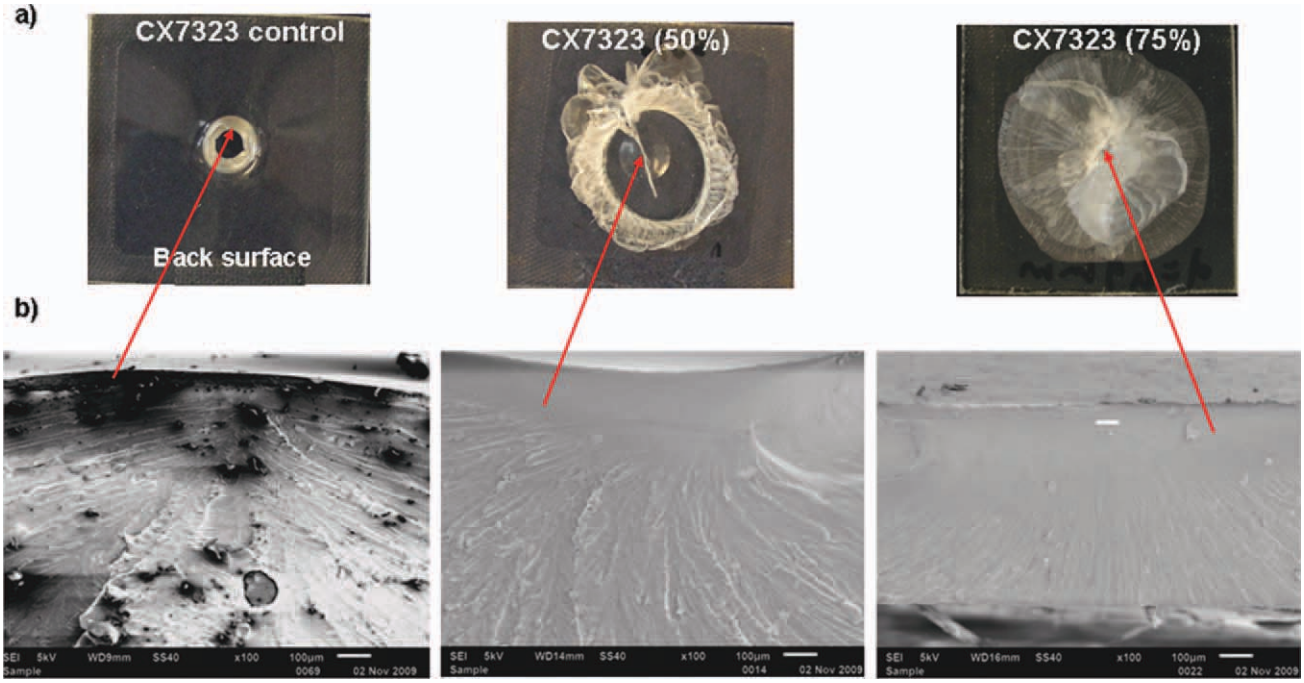

Figure 12 Fracture damage zone comparison of TROGAMID rolled to different thickness reductions. The damage zones were observed with SEM on the cross section of the center cracks where the fracture was first initiated. [Color figure can be viewed in the online issue, which is available at wileyonlinelibrary.com.]

the ND. As a result, nylon 6/6 (75%) again exhibited brittle failure with fracture occurring in the elastic region.

Effect of orientation on the puncture fracture mechanisms

The fracture damage zones of TROGAMID with different degrees of orientation are compared in Figure 11. Figure 11(a) shows the top-view image of the damage zones, and Figure 11(b) gives the cross-sectional images of the damage zones. The top-view image shows that the unoriented TROGAMID control failed by a ductile hole enlargement type fracture with the material ahead of the puncture tip bulging out from the distal surface and conforming to the shape of the puncture tip.[28,29] The fracture occurred from the distal surface and was enlarged to the size of the puncture tip.[30] The cross-sectional view of the damage zone exhibited a large degree of membrane stretching, with material bulging out on the distal surface and with the sample thickness reduced to around one-third of the original sample thickness from the membrane stretching. With TROGAMID rolled to a 50% thickness reduction, the top-view image of the damage zone showed a dent from the localized plastic deformation and a crack fracture in the center of the dent. The center crack was observed to have propagated to the contact area periphery, forming a ring crack. The cross-sectional view of the ring crack showed that it occurred at an oblique angle to the sample surface; this suggested that the ring crack was a result of bending stress from the impact center. The thickness of the puncture center was reduced only by about 25% in TROGAMID CX7323 (50%); this indicated a decrease of ductility with orientation. In TROGAMID rolled to a 50% thickness reduction, the polymer chains were stretched by rolling orientation, which resulted in a decrease of ductility, as stretched polymer chains showed less relaxation of chain clusters.[13] The decrease of ductility led to earlier fracture, faster crack propagation, and the ability of the center crack to propagate to outside the puncture tip contact area and form the peripheral ring crack. In further oriented TROGAMID CX7323 (75%), the top-view image of the damage zone exhibited a center crack on the distal surface and numerous fine radial cracks propagating from the impact center. The cross-sectional image showed that the center crack did not propagate through the whole sample thickness, and the sample failed by delamination instead. The sample showed very little thickness reduction from the puncture deformation; this indicated a further decrease of ductility with orientation. The change of the failure mechanism with orientation from center crack propagation to delamination was attributed to the highly anisotropic structure in CX7323 (75%) as a result of polymer chains becoming more and more stretched in the RD.

The fracture surface scanning electron micrographs of the center crack of the TROGAMID

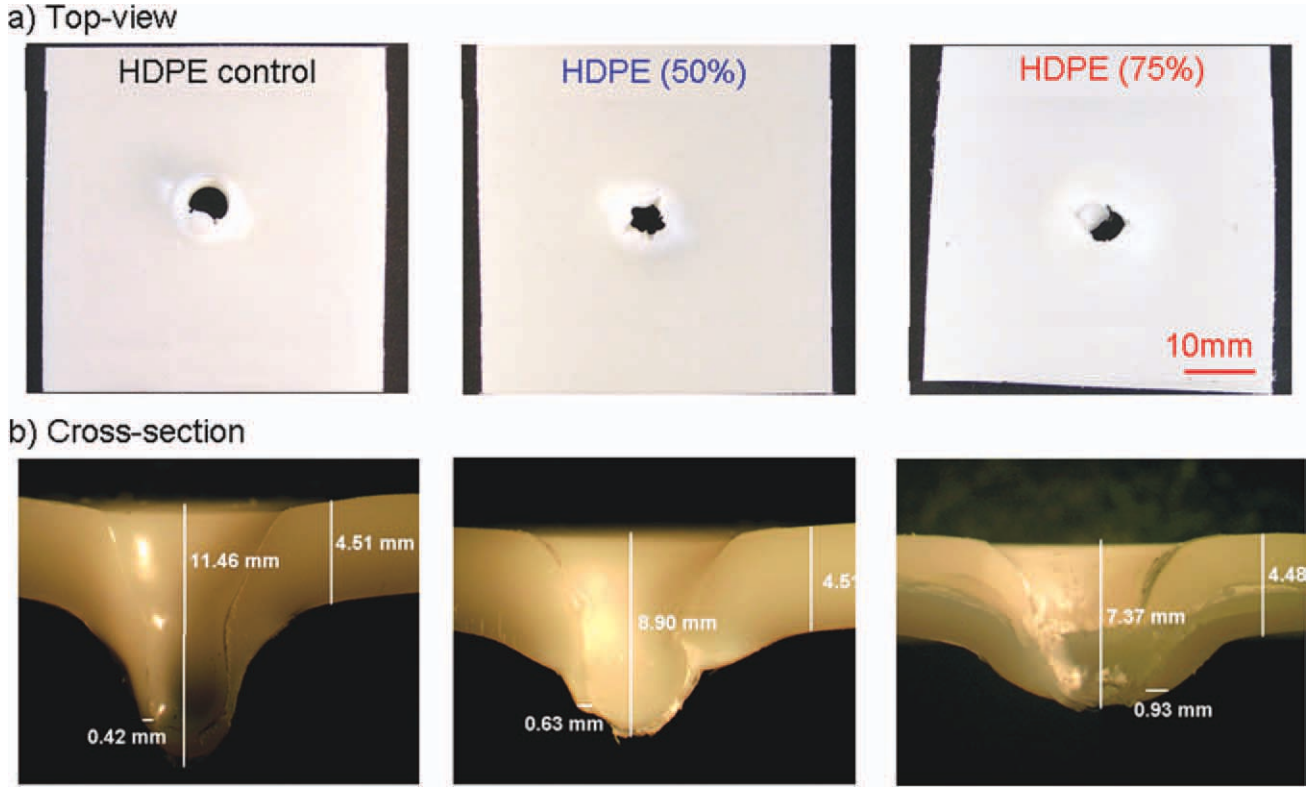

Figure 13 Effect of orientation on the puncture fracture damage zones of HDPE: (a) top view and (b) cross-sectional view of the puncture damage zone. [Color figure can be viewed in the online issue, which is available at wileyonlinelibrary.com.]

samples are shown in Figure 12. For the unoriented TROGAMID CX7323 control, the fracture surface showed extensive riblike flow lines propagating from the crack nucleation center. Contraction of the sides was also observed between the flow lines; this indicated that the fracture was ductile. This type of fracture surface resembled the ductile fracture surface of polycarbonate under notched three-point bending.[31] With material bulging out to form a stretched membrane ahead of the puncture tip, the crack was initiated on the top of the membrane under tensile stress. Once the crack was formed, it acted as a notched tip opening, and the crack propagated under plane stress conditions. In TROGAMID CX7323 (50%), the fracture surface exhibited a large mirrorlike area, which was followed by a rough region of rib marks, characteristic of fast crack propagation. No sucking-in of the sides was discernable; this suggested that it was more of a plane–strain failure. The fracture surface of TROGAMID CX7323 (75%) was similar to that of CX7323 (50%), except the rib marks were finer than in CX7323 (50%). This indicated that the crack propagation was even faster and that the ductility was further decreased with increasing orientation.

Figure 13(a,b) shows the top view and cross section of the damage zones of HDPE rolled to different thickness reductions, respectively. In the top view of the damage zone, all three HDPE samples, regardless of their degree of orientation, showed ductile hole enlargement type fracture similar to the ductile failure of steel under ballistic impact.[30,32] The material was observed to be stretched out on the distal surface from plastic deformation, and a penetration hole was formed in the center of the plastically deformed area. At −40°C, the test temperature was above the T_g of HDPE, and the polymer chains were in a rubbery state, which allowed plastic deformation of crystals, and all HDPE samples failed by ductile fracture as a result. Whitening of the damage zone was observed, and the whitened area increased in size with increasing orientation. Whitening was attributed to microvoid formation from bending deformation.[33] The increase in whitened area indicated the decrease of ductility with increasing orientation. From the side-view images, all samples showed a large amount of membrane stretching; however, the stretching deformation was observed to decrease with increasing orientation. In oriented HDPE, the polymer chains were already stretched by rolling orientation; thus, the ductility decreased with increasing orientation. Delamination failure was also observed from the damage zone side-view image of HDPE rolled to a 75% thickness reduction. In highly

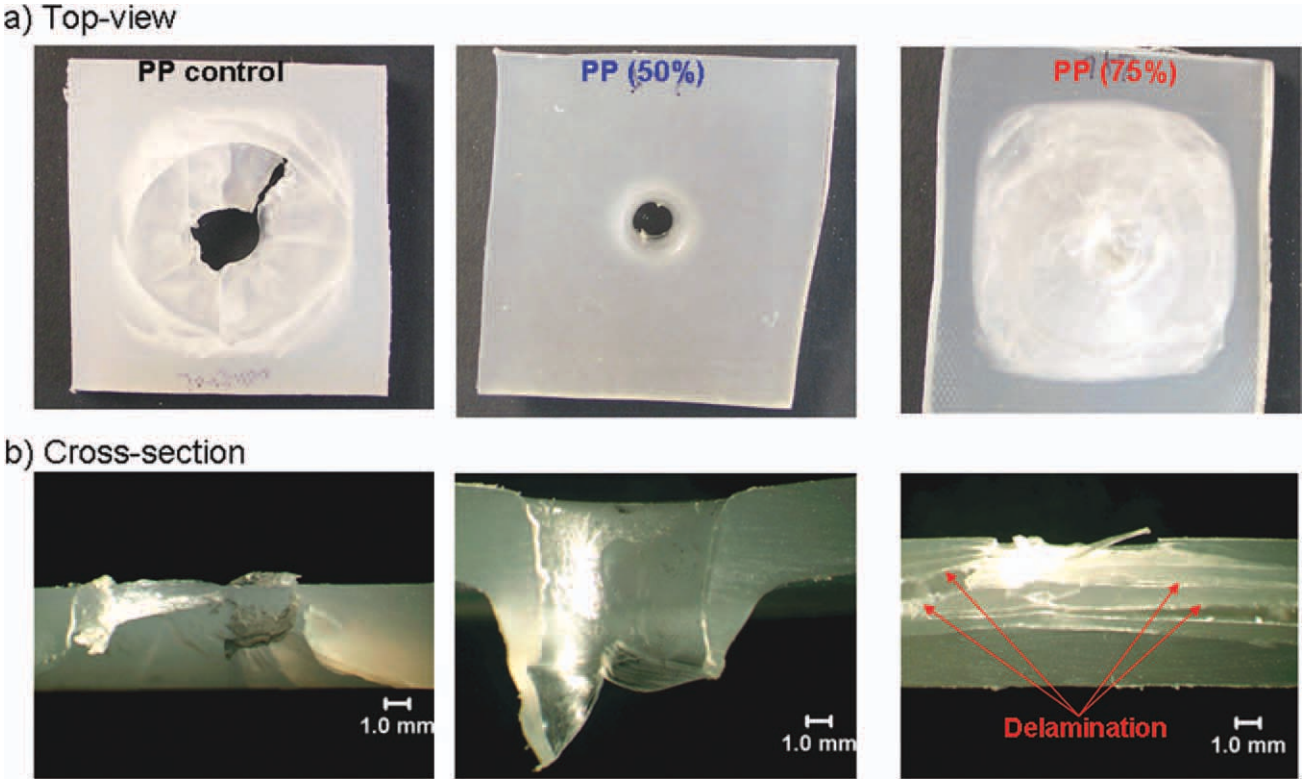

Figure 14 Effect of orientation on the puncture fracture damage zones of PP: (a) top view and (b) cross-sectional view of the damage zone. [Color figure can be viewed in the online issue, which is available at wileyonlinelibrary.com.]

oriented HDPE (75%), orientation changed the isotropic spherulitic structure into a highly anisotropic layeredlike discoid structure,[18,34] which delaminated easily because of the weak planes of this layeredlike structure.

Figure 14 shows the damage zones of PP rolled to different thickness reductions. The top-view image of the unoriented PP control damage zone exhibited a center through-hole with radial cracks propagating from the impact center and a ring crack in the periphery. This type of damage zone was very similar to that of glasses fractured under ballistic impact; this indicated that the PP control failed by brittle fracture.[26,35] In the cross-sectional view of the damage zone, a cone-type crack propagation was observed. A similar result was found in the sphere impact of ceramic with inhomogeneous stress fields, which led to a cone-type crack propagation and which was first discovered by Hertz.[36–38] A ductile hole enlargement failure was observed for PP rolled to a 50% thickness reduction. A center hole the size of the puncture tip was observed in the top view of the damage zone, and the material was seen to be highly stretched to bulge out on the distal surface in the cross-sectional view of the damage zone. During cross-rolling orientation of PP, the randomly distributed lamellae in the spherulitic structure were changed into a tilted lamellar morphology, as shown in a previous schematic. With the chain axis parallel to the puncture shear stress direction, crystals were able to be plastically deformed by chain slip deformation, even though polymer chains were in glassy state. This resulted in a brittle–ductile transition with orientation under the low-temperature puncture of PP. However, a further increase in the PP orientation to a 75% thickness reduction resulted in the failure mechanism changing back to brittle fracture. In the top view of the damage zone, numerous fine radial cracks were observed to propagate from the impact center to the clamp edge, whereas in the cross-sectional view of the damage zone, a delamination failure was witnessed without a through thickness perforation center hole. This indicated that the failure mechanism was transitioned back to a brittle fracture. In further orienting PP, the tilted lamellar structure was replaced by a microfibrillar structure with the chain axis of crystal blocks parallel to the RD; this prohibited the chain slip deformation of crystals. As a result, the sample failed in a brittle manner with delamination in the weak planes from the layered discoidlike structure.

Figure 15 compares the fracture damage zones of nylon 6/6 rolled to different thickness reductions. Similar to PP, the unoriented control of nylon 6/6 also showed brittle fracture with test temperature

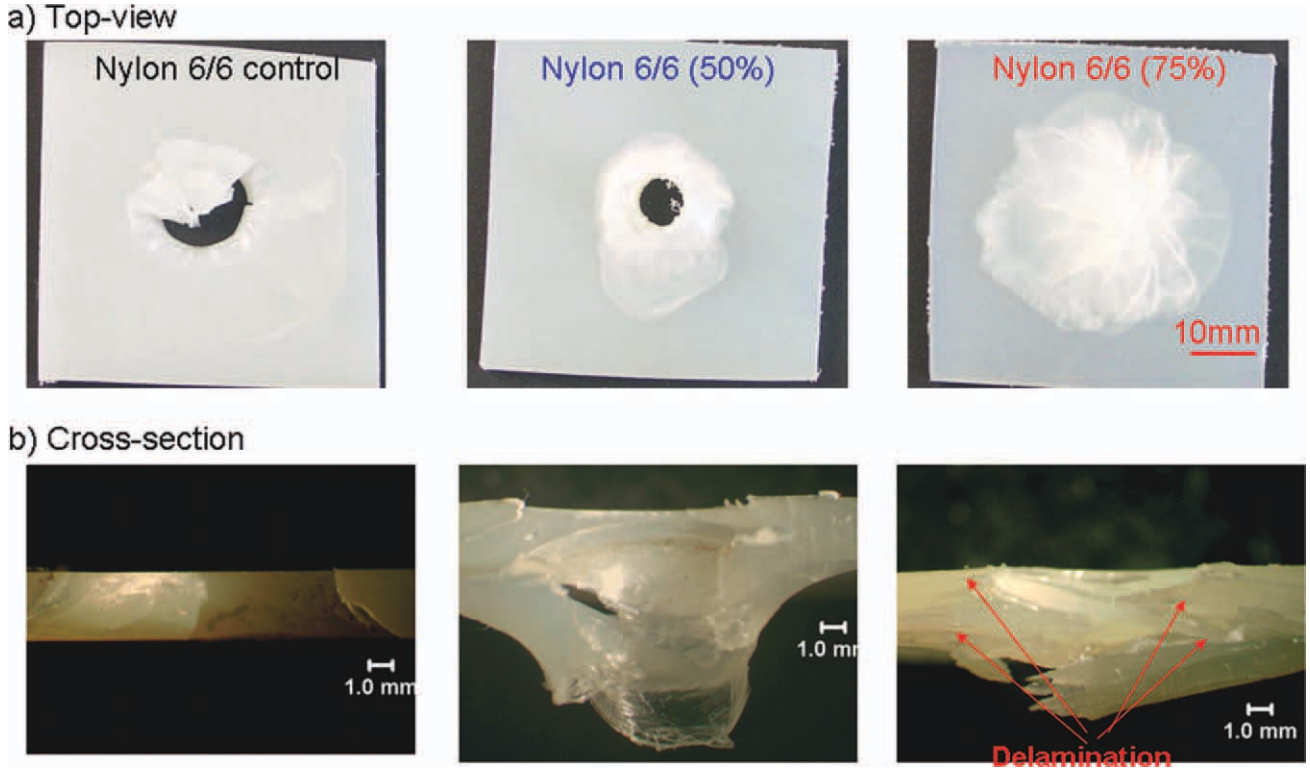

Figure 15 Effect of orientation on the puncture fracture damage zones of nylon 6/6: (a) top view and (b) cross-sectional view of the damage zone. [Color figure can be viewed in the online issue, which is available at wileyonlinelibrary.com.]

below its T_g and the polymer chains in glassy state. Radial cracks propagating from the impact center were observed in the top view of the damage zone, whereas cone cracking was observed in the cross-sectional view of the damage zone. With nylon 6/6 rolled to a 50% thickness reduction, the failure mechanism was changed into a ductile hole enlargement failure. A center through-hole was observed in the top view of the damage zone, whereas membrane stretching was observed in the cross-sectional view of the damage zone. Similar to PP, the orientation of nylon 6/6 changed the randomly oriented lamellar structure into a tilted lamellar morphology; this allowed chain slip deformation of crystals with the chain axis parallel to the puncture shear stress direction. With a further increase in the orientation to a 75% rolling thickness reduction, the failure mechanism again was changed back to brittle fracture, as in PP. Fine radial cracks propagating from the impact center were observed in the top view of the damage zone, whereas significant delamination was seen in the side-view image of the damage zone. Similar to PP, the tilted lamellar structure was changed into a microfibrillar structure with chain axis parallel to the RD; this prevented chain slip deformation of crystals and resulted in the brittle fracture of nylon 6/6 rolled to a 75% thickness reduction. The delamination failure could also be attributed to the isotropic spherulitic structure changing into an anisotropic layeredlike discoid structure.

CONCLUSIONS

The microstructural change with orientation by solid-state cross-rolling and its effects on the puncture deformation and fracture mechanism were studied for an amorphous TROGAMID and three crystalline polymers, HDPE, PP, and nylon 6/6. It was found that orientation led to the straightening of polymer chains in the RD in the amorphous TROGAMID. Orientation of amorphous chains in TROGAMID led to a higher slope of the puncture load–displacement curve in the plastic deformation region because of the increased strain-hardening exponent. However, orientation decreased the drawability of the polymer chains and led to a decrease of the fracture displacement. The decreased ductility with orientation changed the failure mechanism from ductile hole enlargement fracture for the unoriented control to a more brittle delamination failure for TROGAMID cross-rolled to a 75% thickness reduction. A similar result was observed for oriented HDPE as orientation led to the alignment of crystal blocks and amorphous tie chains in the RD and decreased the ductility of HDPE. In PP and nylon 6/6, the unoriented controls exhibited a brittle fracture as the puncture test

temperature was below their T_g and amorphous chains were in a glassy state. However, the brittle fracture was transformed into a ductile failure with PP and nylon 6/6 cross-rolled to a 50% thickness reduction. This transition was attributed to the morphology changing from a randomly distributed lamellar structure into a tilted lamellar structure; this allowed the chain slip deformation of crystals with their chain axis parallel to the puncture shear stress. With PP and nylon 6/6 further cross-rolled to a 75% thickness reduction, the morphology was further changed into a layeredlike discoid morphology with the chain axis of the crystal blocks becoming parallel to the RD. The morphological transformation prevented the chain slip deformation of crystals, as the chain axis became normal to the puncture stress direction. As a result, the puncture failure of PP (75%) and nylon 6/6 (75%) was changed back to brittle fracture, with delamination observed from their layeredlike structure.

References

1. Ward, I. M. Structure and Properties of Oriented Polymers; Applied Science: London, 1975.
2. Ajji, A.; Dumoulin, M. J Appl Polym Sci 2006, 102, 3391.
3. Bartczak, Z. J Appl Polym Sci 2002, 86, 1396.
4. Bartczak, Z.; Morawiec, J.; Galeski, A. J Appl Polym Sci 2002, 86, 1413.
5. Higashida, Y.; Watanabe, K.; Kikuma, T. ISIJ Int 1991, 31, 655.
6. Hutnik, M.; Argon, A. S.; Suter, U. W. Macromolecules 1993, 26, 1097.
7. Utz, M.; Tomaselli, M.; Ernst, R. R.; Suter, U. W. Macromolecules 1996, 29, 2909.
8. Hadziioannou, G.; Wang, L. H.; Stein, R. S.; Porter, R. S. Macromolecules 1982, 15, 880.
9. Peterlin, A. J Mater Sci 1971, 6, 490.
10. Keller, A.; Pope, D. P. J Mater Sci 1971, 6, 453.
11. Bowen, P. B.; Young, R. J. J Mater Sci 1974, 9, 2034.
12. Lin, L.; Argon, A. S. J Mater Sci 1994, 29, 294.
13. Argon, A. S.; Cohen, R. E. Polymer 2003, 44, 6013.
14. Men, Y.; Strobl, G. Macromolecules 2003, 36, 1889.
15. Brady, T. E.; Yeh, G. S. Y. J Appl Phys 1971, 42, 4622.
16. Sova, M.; Raab, M.; Slizova, M. J Mater Sci 1993, 28, 6516.
17. Snyder, J.; Hiltner, A.; Baer, E. J Appl Polym Sci 1994, 52, 217.
18. Yang, Y.; Keum, J.; Zhou, Z.; Thompson, G.; Hiltner, A.; Baer, E. J Appl Polym Sci 2010, 118, 659.
19. Yang, Y.; Thompson, G.; Song, J.; Hiltner, A.; Baer, E. J Appl Polym Sci 2009, 112, 163.
20. Murthy, N. S.; Minor, H.; Bednarczyk, C.; Krimm, S. Macromolecules 1993, 26, 1712.
21. Gezovich, D. M.; Geil, P. H. J Mater Sci 1971, 6, 531.
22. Pluta, M.; Bartczak, Z.; Galeski, A. Polymer 2000, 41, 2271.
23. Lin, Y. J.; Dias, P.; Chen, H. Y.; Hiltner, A.; Baer, E. Polymer 2008, 49, 2578.
24. Baucom, J. N.; Zikry, M. A. J Compos Mater 2003, 37, 1651.
25. Mines, R. A. W.; Roach, A. M.; Jones, N. Int J Impact Eng 1999, 22, 561.
26. Cunha, T.; Wu, J.; Peitl, O.; Fokin, V.; Znotto, E.; Iannucci, L.; Boccaccini, A. Adv Eng Mater 2007, 9, 191.
27. Galeski, A. Prog Polym Sci 2003, 28, 1643.
28. Abdullah, M. R.; Cantwell, W. J. Compos Sci Technol 2006, 66, 1682.
29. Backman, M. E.; Goldsmith, W. Int J Eng Sci 1978, 16, 1.
30. Borvik, T.; Langseth, M.; Hopperstad, O.; Malo, K. Int J Impact Eng 1999, 22, 855.
31. Yee, A. F. J Mater Sci 1977, 12, 757.
32. Ubeyli, M.; Yildirim, R.; Ogel, B. Mater Des 2007, 28, 1257.
33. Liu, Y.; Truss, R. W. J Polym Sci Part B: Polym Phys 1994, 32, 2037.
34. Pan, S.; Tang, H.; Hiltner, A.; Baer, E. Polym Eng Sci 1987, 27, 869.
35. Walley, S. M.; Field, J. E.; Blair, P. W.; Milford, A. J. Int J Impact Eng 2004, 30, 31.
36. LaSalvia, J.; Normandia, M. J.; Mackenzie, D. E.; Miller, H. T. Ceram Eng Sci Proc 2005, 26, 193.
37. Chaudhri, M. M.; Chen, L. Y. J Mater Sci 1989, 24, 3441.
38. Lawn, B. R. J Am Ceram Soc 1998, 81, 1977.